

Randomly Diluted e_g Orbital-Ordered Systems

T. Tanaka, M. Matsumoto, and S. Ishihara

Department of Physics, Tohoku University, Sendai 980-8578, Japan

(Dated: July 26, 2021)

Dilution effects on the long-range ordered state of the doubly degenerate e_g orbital are investigated. Quenched impurities without the orbital degree of freedom are introduced in the orbital model where the long-range order is realized by the order-from-disorder mechanism. It is shown by the Monte-Carlo simulation and the cluster-expansion method that a decrease in the orbital-ordering temperature by dilution is remarkable in comparison with that in the randomly diluted spin models. Tilting of orbital pseudo-spins around impurity is the essence of this dilution effects. The present theory provides a new view point for the recent resonant x-ray scattering experiments in $\text{KCu}_{1-x}\text{Zn}_x\text{F}_3$.

PACS numbers: 75.30.-m, 71.23.-k, 71.10.-w, 78.70.-g

Impurity effects on the long-range ordered state are one of the attractive themes in recent study of correlated electron systems [1]. A small amount of non-magnetic impurities dramatically destroy the superconductivity in cuprates, and induce the antiferromagnetic long-range order in the low-dimensional quantum spin-liquids. Doped impurities also cause striking effects on the charge- and orbital-orders; substitution of Cr ions for Mn in colossal magnetoresistive (CMR) manganites immediately destroys the charge-orbital orders [2]. Origin of CMR itself is studied from the view point of randomness and/or percolation [3].

Recently, the dilution effects in KCuF_3 by substituting Zn for Cu is reported experimentally by Tatami *et al.* [4]. A Cu^{2+} ion in the cubic-crystalline field shows the $t_{2g}^6 e_g^3$ configuration which has the e_g orbital degree of freedom. The Cu ions in the perovskite crystal form the three-dimensional (3D) simple-cubic (SC) lattice, and exhibit the long-range orbital order (OO) in room temperatures, where the $d_{y^2-z^2}$ - and $d_{z^2-x^2}$ -like orbitals are aligned with momentum $\mathbf{Q} = (\pi, \pi, \pi)$. Since the five d orbitals are fully occupied in Zn^{2+} , substitution of Zn for Cu corresponds to dilution of orbital. The resonant x-ray scattering (RXS) studies in $\text{KCu}_{1-x}\text{Zn}_x\text{F}_3$ reveal that a decrease in the orbital-ordering temperature (T_{OO}) by dilution is remarkable in comparison with the randomly diluted magnets, and OO disappears around $x = 0.5$, as shown in the inset of Fig. 1. These observations may not be explained by the conventional percolation scenario; the site-percolation threshold in 3D SC lattice is $x_c (\equiv 1 - p_c) = 0.69$ which is applicable well to the several diluted magnets such as $\text{KMn}_{1-x}\text{Mg}_x\text{F}_3$ [5, 6].

We examine, in this Letter, the dilution effects on the long-range order of the e_g orbital degree of freedom. As well known, the doubly degenerate e_g orbital is treated by the pseudo-spin (PS) operator with a magnitude of $1/2$; $\mathbf{T}_i = \frac{1}{2} \sum_{\gamma, \gamma', s} d_{i\gamma s}^\dagger \sigma_{\gamma\gamma'} d_{i\gamma' s}$ where $d_{i\gamma s}$ indicates the annihilation operator of a hole with spin s and orbital γ at site i , and σ is the Pauli matrices. A shape of the electronic orbital is described by an angle θ of the PS vector as $|\theta\rangle = \cos(\theta/2)|d_{3z^2-r^2}\rangle + \sin(\theta/2)|d_{x^2-y^2}\rangle$. For example, $\theta = 0, 2\pi/3$ and $4\pi/3$ correspond to the $d_{3z^2-r^2}, d_{3x^2-r^2}$, and $d_{3y^2-r^2}$ orbitals, respectively, and $\theta = \pi/3, \pi$ and $-\pi/3$ to $d_{y^2-z^2}, d_{x^2-y^2}$, and $d_{z^2-x^2}$,

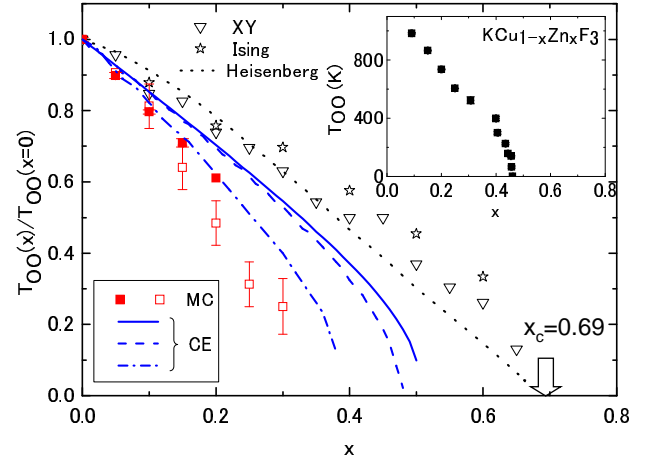


FIG. 1: Impurity concentration dependence of the normalized orbital-ordering temperature $T_{\text{OO}}(x)/T_{\text{OO}}(x=0)$. The calculated results by the MC method are shown by the closed- and open-red squares (see text), and those by the CE method for the one- and two-site clusters are shown by the bold- and broken-blue lines, respectively. The results by the CE method where the PS operator is treated as a classical vector are shown by the one-point chain line (blue). For comparison, T_{N} in the XY (reverse-triangles) and Ising (stars) models by the MC method, and that in the Heisenberg model (dotted line) by the CE method are also shown. The inset shows the Zn concentration dependence of T_{OO} in $\text{KCu}_{1-x}\text{Zn}_x\text{F}_3$ obtained by the XRS experiments [4].

respectively. As shown below, the Hamiltonian for the diluted orbital system is described by the PS operators and seems to be on the same footing with the spin models. However, the obtained results are qualitatively different from the diluted magnets. The main results are shown in Fig. 1. The impurity-concentration x dependences of T_{OO} , calculated by the two different methods, show rapid decreases in comparison with that in the spin models. The results can explain the experimentally discovered anomalous dilution effects in $\text{KCu}_{1-x}\text{Zn}_x\text{F}_3$ [4].

The model Hamiltonian adopted here describes the orbital interaction between the nearest-neighbor (NN) Cu sites in a

3D SC lattice:

$$\mathcal{H} = 2J \sum_{\langle ij \rangle} \tau_i^l \tau_j^l \varepsilon_i \varepsilon_j, \quad (1)$$

where $J(> 0)$ is the interaction, and $\langle ij \rangle$ indicates a pair of the NN sites along the direction $l(=x, y, z)$. The operator τ_i^l depends explicitly on the bond direction and is defined by a linear combination of the PS operators as

$$\tau_i^l = \cos\left(\frac{2\pi}{3}n_l\right) T_{iz} + \sin\left(\frac{2\pi}{3}n_l\right) T_{ix}, \quad (2)$$

with $(n_x, n_y, n_z) = (1, 2, 3)$. The quenched impurities without the orbital degree of freedom are introduced by ε_i taking one and zero for Cu and Zn, respectively.

The Hamiltonian in Eq. (1) without impurities ($\varepsilon_i = 1$ for $\forall i$) does not concern an origin of the interaction, i.e. the electronic and/or phononic interactions. In the electronic view point, this is derived by the generalized-Hubbard model with the e_g orbital degree of freedom. Through the perturbational expansion with respect to the NN electron transfer t , the spin-orbital superexchange model is obtained [7, 8]; $\mathcal{H}_{ST} = -2J_1 \sum_{\langle ij \rangle} (\frac{3}{4} + \mathbf{S}_i \cdot \mathbf{S}_j) (\frac{1}{4} - \tau_i^l \tau_j^l) - 2J_2 \sum_{\langle ij \rangle} (\frac{1}{4} - \mathbf{S}_i \cdot \mathbf{S}_j) (\frac{3}{4} + \tau_i^l \tau_j^l + \tau_i^l + \tau_j^l)$. Here, \mathbf{S}_i is the spin operator at site i with magnitude of 1/2, and $J_1(=t^2/(U-3I))$ and $J_2(=t^2/U)$ are the superexchange interactions with the on-site intra-orbital Coulomb interaction U and the exchange interaction I . Since the Néel temperature (T_N) in $\text{KCu}_{1-x}\text{Zn}_x\text{F}_3$ is far below T_{OO} in a whole range of x [4], taking $\mathbf{S}_i \cdot \mathbf{S}_j = 0$ is a good assumption, and Eq. (1) with $J = \frac{3}{4}J_1 - \frac{1}{4}J_2$ is obtained. In the phononic view point, the orbital model is derived based on the cooperative Jahn-Teller (JT) effects. Start from the linear JT coupling Hamiltonian $\mathcal{H}_{JT} = g \sum_{i,m=(x,z)} Q_{im} T_{im}$ with the vibrational modes Q_{im} ($m=x, z$) in a F_6 octahedron, and the lattice potential K between NN Cu-F bonds. After rewriting Q_{im} by the phonon coordinates $\mathbf{q}_{\mathbf{k}}$, we obtain Eq. (1) with $J = 2g^2/(9K)$ by integrating out $\mathbf{q}_{\mathbf{k}}$ [9, 10]. A sign of J is positive in both the two processes. A unique aspect of the orbital model to be noticed here is that the explicit form of the interaction depends on the bond direction l ; the interactions are $T_{iz}T_{jz}$ for $l=z$, and $[-\frac{1}{2}T_{iz} + (-)\frac{\sqrt{3}}{2}T_{ix}][-\frac{1}{2}T_{jz} + (-)\frac{\sqrt{3}}{2}T_{jx}]$ for $l=x(y)$. When we focus on one direction l , the staggered alignment of the $d_{3l^2-r^2}$ and $d_{m^2-n^2}$ orbitals with $(l, m, n) = (x, y, z), (y, z, x)$ and (z, x, y) is favored. In a 3D SC lattice with and without impurities, the stable orbital configurations are non-trivial.

We have attacked this issue by the numerical approach together with the analytical one, i.e. the classical Monte-Carlo (MC) simulation, and the cluster expansion (CE) method. In the MC method, the PS operator is treated as a classical vector defined in the $T_x - T_z$ plane. The MC calculations have been performed for the cubic $L \times L \times L$ lattice ($L = 10 \sim 18$) with the periodic-boundary condition. For each sample, 30,000MC steps are spent for measurement after 8,000MC steps for thermalization. The physical quantities are averaged over 20 \sim 80 MC samples at each parameter set. We adopt the CE method proposed in Ref. [11], where the fluctuations of the

effective fields are determined with the order parameter, self-consistently. Even in the two-site clusters, this CE method provides good values for x_c and the Curie temperature T_C at $x=0$ for Ising and Heisenberg models [11].

First, we show the results without impurities. It is known that, in the orbital model [Eq. (1)] at $x=0$, there is a macroscopic number of degeneracy in the mean-field (MF) ground state [12, 13, 14, 15, 16]. These are classified into the two; (i) One of the MF solutions is the staggered-type OO with two sublattices, termed A and B , and the momentum $\mathbf{Q} = (\pi, \pi, \pi)$. The orbital angles in the sublattices are $(\theta_A/\theta_B) = (\theta/\theta + \pi)$ for any value of θ . Such continuous-rotational symmetry is unexpected from Eq. (1). (ii) Consider an OO with $\mathbf{Q} = (\pi, \pi, \pi)$ and $(\theta_A/\theta_B) = (\theta_0/\theta_0 + \pi)$, and focus on one direction in a 3D SC lattice, e.g. the z direction. The MF energy is not changed by changing $(\theta_0/\theta_0 + \pi) \rightarrow (-\theta_0/-\theta_0 - \pi)$ in each layer in the xy plane. Both the types of degeneracy are understood from the momentum representation of Eq. (1): $\mathcal{H} = \sum_{\mathbf{k}} \psi_{\mathbf{k}}^l \hat{J}(\mathbf{k}) \psi_{\mathbf{k}}$ with $\psi_{\mathbf{k}} = [T_{z\mathbf{k}}, T_{x\mathbf{k}}]$ and the 2×2 matrix $\hat{J}(\mathbf{k})$. By diagonalizing $\hat{J}(\mathbf{k})$, we obtain the eigen values $J_{\pm}(\mathbf{k}) = 2J[-c_x - c_y - c_z \pm \sqrt{c_x^2 + c_y^2 + c_z^2 - c_x c_y - c_y c_z - c_z c_x}]$ with $c_l = \cos(\pi k_l/a)$ [17]. $J_-(\mathbf{k})$ has its minimum along $(\pi, \pi, \pi) - (0, \pi, \pi)$ and other three-equivalent directions. A lifting of the degeneracy in the orbital model is discussed in Refs. [15, 16] by the spin-wave analyses. Here we show the lifting of the degeneracy by the MC method. In Fig. 2 (a), number of data obtained in the simulation is plotted as a function of the orbital angle θ in the staggered-type OO with $(\theta_A/\theta_B) = (\theta/\theta + \pi)$. It is shown that the type-(i) orbital degeneracy is lifted; θ is confined to the three discontinuous values of 0, $2\pi/3$ and $4\pi/3$. The inset shows number of data as function of the orbital-order parameter M_O at $\mathbf{Q} = (\pi, \pi, \pi)$ defined as $M_O^2 = \sum_{m=x,z} \langle T_{\mathbf{Q}m} T_{-\mathbf{Q}m} \rangle$ with $T_{\mathbf{k}m} = \frac{1}{N} \sum_i e^{i\mathbf{k} \cdot \mathbf{r}_i} T_{im}$. Most of the data show $M_O = 0.5$, implying that the ordering pattern is of a staggered type, and the type-(ii) degeneracy is also lifted.

We have performed the finite-size scaling analyses in the MC simulation to determine T_{OO} . The correlation length ξ is calculated by the second-moment method in the PS correlation function for several sizes L . In Fig. 2(b), we demonstrate the scaling plot for ξ/L as a function of $(T - T_{\text{OO}})L^{1/\nu}$ at $x=0$. The scaling analyses work quite well for $L=10, 12$ and 14. T_{OO} and the exponent ν are determined through the least-square fitting by the polynomial expansion and obtained as $T_{\text{OO}}/J = 0.344 \pm 0.002$ and $\nu = 0.69 - 0.81$, although statistical errors are not enough to obtain the precise value of ν . Even in the diluted case [see the inset of Fig. 2(b)], the precision is enough to determine $T_{\text{OO}} [= (0.248 \pm 0.003)J$ for $x=0.15$]. Beyond $x=0.15$, the scaling analyses do not work well.

In Fig. 3(a), the temperature dependence of the normalized-order parameter $\frac{1}{1-x} M_O [= m_O(x, T)]$ are presented. First, focus on the region of $x \leq 0.15$. As expected, $m_O(x=0, T)$ abruptly increases at T_{OO} and is saturated to 0.5 at $T \rightarrow 0$. By doping impurity, $m_O(x, T)$ does not reach 0.5 even far below

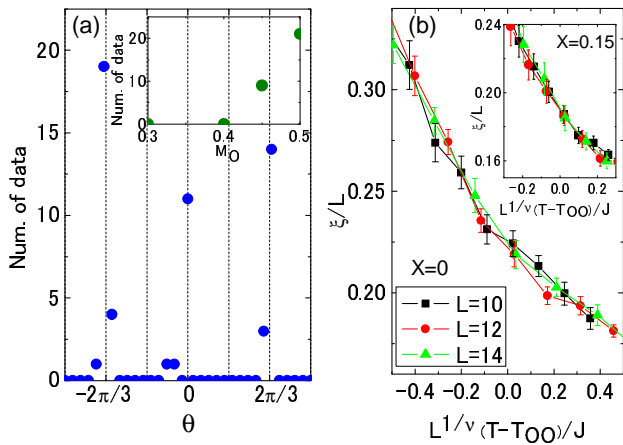


FIG. 2: (a) A MC data distribution for the orbital angle θ in the staggered-type orbital order at $x = 0$. The inset shows a data distribution of the order parameter M_O at $x = 0$. (b) The finite-size scaling for the correlation length ξ/L as functions of $L^{1/\nu}(T - T_{OO})/J$ at $x = 0$. The inset shows the scaling plot at $x = 0.15$.

T_{OO} , and $m_O(x \neq 0, T \rightarrow 0)$ gradually decreases with increasing x . Although the system sizes are not sufficient to estimate $m_O(x, T)$ in the thermodynamic limit, $m_O(x \neq 0, T \rightarrow 0)$ does not show the smooth convergence to 0.5 in contrast to the diluted spin models. Beyond $x = 0.15$, the situation is changed qualitatively; in spite of the fact that $m_O(x, T)$ grows around a certain temperature (e.g. $\sim 0.18J$ at $x = 0.2$), $m_O(x, T \rightarrow 0)$ becomes small abruptly and decreases weakly with increasing L . Anomalies in the specific heat and the susceptibility around this temperature become weak, and some of the physical quantities, e.g. $N_O \equiv \sum_{m=x,z} \langle T_{Qm} \rangle^2$ with $\mathbf{Q} = (\pi, \pi, \pi)$, depend on the initial states in the MC simulation. It seems that the orbital correlation grows up below this temperature, but the long-range order does not. We suppose that a possible orbital state in this region is a short-range ordered state or a glass state [18], although we do not identify this phase correctly at the present stage. Thus, in $x > 0.15$, a temperature where $dm_O(x, T)/dT$ in $L = 18$ takes a maximum is interpreted to be the cross-over and/or glass-transition temperature. Above $x = 0.3$, estimation of T_{OO} becomes severe, because of the weak temperature dependence of $m_O(x, T)$. Thus, as a supplementary information of the ordering temperature, we calculate a temperature \tilde{T}_{OO} where dN_O/dT takes a maximum, and consider its full width at half maximum as an error. The initial state in the calculation for \tilde{T}_{OO} is assumed to be the ordered state, although the initial-state dependence of \tilde{T}_{OO} is much weaker than that of the N_O amplitude.

The x dependences of T_{OO} (and \tilde{T}_{OO}) presented in Fig. 1 are obtained by the MC (filled-red squares) and CE (blue lines) methods introduced above. For comparison, the x dependences of T_N in the spin models are plotted. \tilde{T}_{OO} s are also shown by the open-red squares. Starting to dope impurities in the orbital model, decrease of T_{OO} is more remarkable than

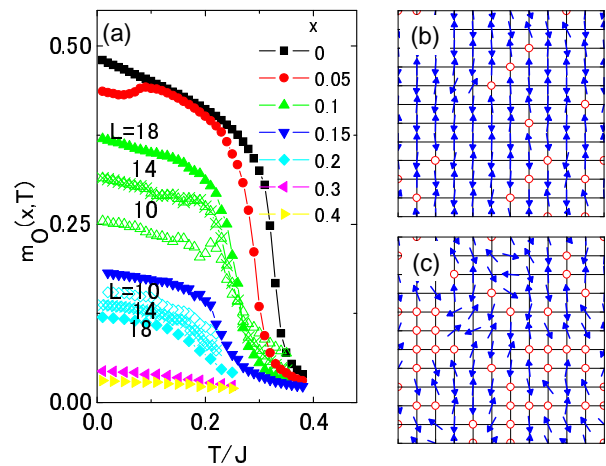


FIG. 3: (a) Temperature dependence of the normalized order parameter $m_O(x, T) [= M_O/(1-x)]$ for various x and L . (b) A snapshot in the MC simulation for the PS configuration at $x = 0.1$. Open circles indicate the impurities. (c) A snapshot at $x = 0.3$.

that of T_N in the spin models. Around $x = 0.15$, the clear transition to the long-range order becomes obscure, explained above. \tilde{T}_{OO} s obtained by N_O are close to T_{OO} below $x = 0.2$, and decrease smoothly up to $x = 0.3$, although the critical x , where \tilde{T}_{OO} disappears, is not determined due to large statistical errors. A rapid decrease of T_{OO} is also obtained by the CE method. It is seen that difference between the calculated $T_{OO} - x$ curves for the cluster sizes $N_C = 1$ (bold line) and 2 (broken like) is within a few percent. T_{OO} in the CE method disappears around $x = 0.5$ being much smaller than $x_c = 0.69$ for the 3D SC lattice. We also calculate T_{OO} in the CE method where the quantum PS operators are replaced by the classical vectors. The calculated results plotted by the one-point chain line are close qualitatively to the $T_{OO}(\tilde{T}_{OO}) - x$ curve obtained by the classical MC method.

Now we introduce the physical picture of the diluted orbital-ordered state. The real-space configurations of the orbital PSs help us to understand the calculated $T_{OO} - x$ curve. The MC snapshots of the PSs on a plane are shown in Figs. 3(b) and (c) for $x=0.1$ and 0.3, respectively. The staggered-type OO with the orbital angles $(\theta_A/\theta_B) = (0/\pi)$ is seen in the back-ground of Fig. 3(b). At the neighboring sites of the impurities indicated by the open circles, tiltings of the PS vectors are observed. Disturbing the PS configuration from $(0/\pi)$ becomes violent at $x = 0.3$. These observations are caused by the local-symmetry breaking by dilution. Consider the orbital state at a neighboring site of an impurity on the x axis. On account of the impurity, one of the interactions along x vanishes. Since the interaction depends on the bond direction explicitly in the orbital model, the PS at this site tilts to gain the interaction energies for other five bonds. This is the essence of the diluted orbital systems and is in contrast to

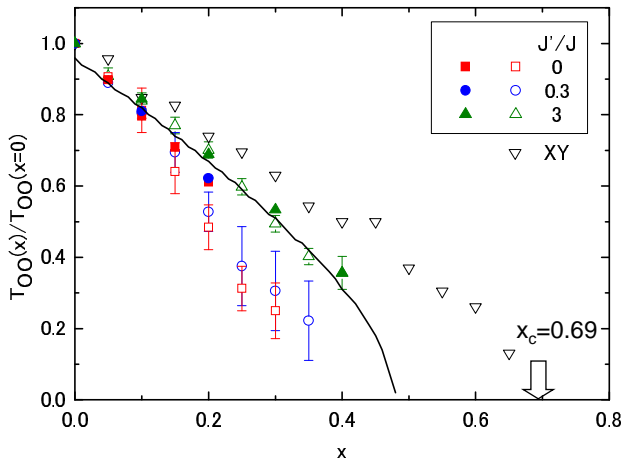


FIG. 4: Impurity concentration dependence of the normalized orbital-ordering temperature $T_{OO}(x)/T_{OO}(x=0)$ with the higher-order JT coupling. The squares, circles and triangles indicate $T_{OO}(x)/T_{OO}(x=0)$ at $J'/J=0, 0.3$ and 3 , respectively. T_{OO} s indicated by the open and filled symbols are defined in the text. For comparisons, T_N of the XY model (reverse triangles), and T_{OO} at $J'/J=0$ by the CE method (bold line) are also plotted.

the conventional diluted spin models. To check roles of this PS tilting on the anomalous $T_{OO}-x$ curve, we have performed the MC calculations in the model where the available orbital angles in the T_z-T_x plane are restricted to a few states. The obtained $T_{OO}-x$ curve is similar to that in the spin models; the tilting of PSs is confirmed to be the origin of the rapid decrease of T_{OO} .

Finally, to compare the present theory with the experiments in $KCu_{1-x}Zn_xF_3$, more directly, we introduce the higher-order JT coupling. From the RXS experiments [4] and the lattice distortion in $KCuF_3$ [19], the OO in $KCuF_3$ is expected to be the $d_{y^2-z^2}/d_{z^2-x^2}$ -type; the cant-type OO with the orbital angles $(\theta'/-\theta)$ ($\theta \sim \pi/3$) and $\mathbf{Q} = (\pi, \pi, \pi)$. To reproduce this type of OO, the higher-order JT coupling is required, $\mathcal{H}_{JT} = g' \sum_i \{ (Q_{iz}^2 - Q_{ix}^2) T_{iz} - 2Q_{iz}Q_{ix}T_{ix} \}$ which provides the anisotropy in the PS space. Here we treat approximately this term based on the theory of the cooperative JT effects. By rewriting $Q_{ix(z)}$ by the phonon coordinates \mathbf{q}_k , and integrating out \mathbf{q}_k , the interaction between orbitals at the different three-neighboring sites is obtained: $\mathcal{H}' = J' \sum_{\langle ijk \rangle} \{ (T_{iz}T_{jz} + T_{ix}T_{jx}) T_{kz} - 2T_{iz}T_{jz}T_{kx} \} \varepsilon_i \varepsilon_j \varepsilon_k$. Here, $J' = (16g'g^2)/(9K^2)$ is the coupling constant and $\langle ijk \rangle$ indicates a sum of the neighboring three sites. The MF energy of \mathcal{H}' is proportional to $\frac{J'}{8} \cos 3\theta$ implying the anisotropy. A value of g' for a Cu^{2+} ion was estimated by the adiabatic potential barrier in a molecule [20] and corresponds to J' being about $0.3J$. We have performed the MC calculations in the model of $\mathcal{H} + \mathcal{H}'$, and observed that the cant-type OO at $x=0$ is realized. The doping dependences of T_{OO} (and \tilde{T}_{OO}) with including \mathcal{H}' are presented in Fig. 4 for $J'/J=0.3$ and 3 . The filled and open symbols are for T_{OO} and \tilde{T}_{OO} , respectively, which are

obtained by the same ways with those in Fig. 1. With increasing J' , the $T_{OO}(\tilde{T}_{OO})-x$ curves approach to those for the spin models, because the anisotropy suppresses the tilting of PSs. However, we confirm that the rapid reduction of T_{OO} by dilution survives even in the calculation with the realistic value of J' , and is consistent with the RXS experimental results shown in the inset of Fig. 1.

In summary, we have investigated the dilution effects on the long-range order of the e_g orbital degree of freedom. We confirm, by both the MC and CE methods, that T_{OO} decreases rapidly with doping, in comparison with the diluted magnets. The tilting of the orbital PSs around impurities, which is distinguished qualitatively from the spin models, is the essence for the rapid decrease of T_{OO} . The present theory provides a new view point for the recent experiments in a diluted orbital systems of $KCu_{1-x}Zn_xF_3$. A broad peak profile observed by the RXS experiments [4] may be attributed to the orbital tilting around impurities. Observations of the tilting by the scanning-tunneling microscope and/or the scanning-electron microscope are a direct check for the present results.

Authors would like to thank Y. Murakami for valuable discussion and permission to use the experimental data before publication. This work was supported by KAKENHI from MEXT, NAREGI and CREST. Part of the numerical calculation was performed by the supercomputers in IMR, Tohoku Univ., and ISSP, Univ. of Tokyo. T. T. appreciates a financial support from Research Fellowship of JSPS. M. M. thanks S. Todo for helpful discussions.

-
- [1] S. Maekawa *et al.*, *Physics of Transition Metal Oxides*, (Springer Verlag, Berlin, 2004), and references therein.
 - [2] A. Barnabe *et al.*, *Appl. Phys. Lett.* **71**, 3907 (1997).
 - [3] M. Uehara *et al.*, *Nature*, **399**, 560 (1999).
 - [4] N. Tatami, S. Niioka, and Y. Murakami, (in preparation).
 - [5] R. B. Stinchcombe, in *Phase Transition in Critical Phenomena*, Vol. 7, edited by C. Domb and J. L. Lebowitz, (Academic Press, London, 1983).
 - [6] D. J. Breed *et al.*, *J. Appl. Phys.* **41**, 1267 (1970).
 - [7] K. I. Kugel *et al.*, *Sov. Phys. JETP* **37**, 725 (1973).
 - [8] S. Ishihara *et al.*, *Phys. Rev. B* **55**, 8280 (1997).
 - [9] J. Kanamori, *J. Appl. Phys.* **31**, 14S (1960).
 - [10] S. Okamoto *et al.*, *Phys. Rev. B* **65**, 144403 (2002).
 - [11] H. Mano, *Prog. Theor. Phys.*, **57**, 1848 (1977).
 - [12] L. F. Feiner *et al.*, *Phys. Rev. Lett.* **78**, 2799 (1997).
 - [13] G. Khaliullin *et al.*, *Phys. Rev. B* **56**, R14243 (1997).
 - [14] S. Ishihara *et al.*, *Phys. Rev. B* **62**, 2338 (2000).
 - [15] K. Kubo, *J. Phys. Soc. Jpn.* **71**, 1308 (2002).
 - [16] Z. Nussinov *et al.*, *Euro. Phys. Lett.* **67**, 990 (2004).
 - [17] S. Ishihara *et al.*, *Phys. Rev. B* **56**, 686 (1997).
 - [18] K. Binder *et al.*, *Adv. Phys.* **41**, 547 (1992).
 - [19] K. Hirakawa *et al.*, *J. Phys. Soc. Jpn.* **15**, 2063 (1969).
 - [20] S. Shashkin *et al.*, *Phys. Rev. B* **33**, 1353 (1986).